

Two-Dimensional Coordination Polymers with One-Dimensional Magnetic Chains: Hydrothermal Synthesis, Crystal Structure, and Magnetic and Thermal Properties of $\infty[\text{MCl}_2(4,4'\text{-bipyridine})]$ ($\text{M} = \text{Fe}, \text{Co}, \text{Ni}, \text{Co/Ni}$)

Michael A. Lawandy, Xiaoying Huang, Ru-Ji Wang, Jing Li,* and Jack Y. Lu

Department of Chemistry, Rutgers University, Camden, New Jersey 08102

Tan Yuen and C. L. Lin

Department of Physics, Temple University, Philadelphia, Pennsylvania 19122

Received March 15, 1999

Two-dimensional transition-metal coordination polymers $\infty[\text{MCl}_2(\text{bpy})]$ ($\text{M} = \text{Fe}, \text{Co}, \text{Ni}; \text{Co/Ni}$, $\text{bpy} = 4, 4'$ -bipyridine) have been synthesized in superheated water solutions. The hydrothermal routes resulted in four compounds $\infty[\text{FeCl}_2(\text{bpy})]$ (**I**), $\infty[\text{CoCl}_2(\text{bpy})]$ (**II**), $\infty[\text{NiCl}_2(\text{bpy})]$ (**III**), and $\infty[(\text{Co/Ni})\text{Cl}_2(\text{bpy})]$ (**IV**). Compounds **I–IV** are isostructural and belong to orthorhombic crystal system, space group *Cmmm* (No. 65). Crystal data for **I**: $a = 11.929(2) \text{ \AA}$, $b = 11.447(2) \text{ \AA}$, $c = 3.638(1) \text{ \AA}$, $V = 496.77(18) \text{ \AA}^3$, $Z = 2$. Crystal data for **II**: $a = 11.993(2) \text{ \AA}$, $b = 11.374(2) \text{ \AA}$, $c = 3.611(1) \text{ \AA}$, $V = 492.57(18) \text{ \AA}^3$, $Z = 2$. The structure is a noninterpenetrating two-dimensional network containing transition-metal centers octahedrally coordinated by four bridging chlorine and two bpy ligands at trans positions. The adjacent bpy ligands within a single layer are parallel to each other at a distance of 3.6 \AA . Spontaneous antiferromagnetic ordering was found in all compounds from the magnetic susceptibility $\chi(T)$ measurements under low fields. The transition temperatures are 10.0, 5.0, 8.5, and 7.5 K , for **I**, **II**, **III**, and **IV**, respectively. The μ_{eff} values yielded from fitting the high temperature $\chi(T)$ indicate the high spin states of metal ions. In addition, a metamagnetic transition was observed in the field-dependent magnetization measurement for all four compounds. The magnetic properties observed in this system are attributed to the ferromagnetic intrachain M–M exchange interaction through the Cl_2 bridges along the c axis and the antiferromagnetic interchain interaction between the M ions. TGA studies indicate that all four compounds are thermally stable with an on-set temperature of weight loss greater than $400 \text{ }^\circ\text{C}$.

Introduction

The hydrothermal method¹ is well-known for its effectiveness in promoting crystal growth. When superheated, water behaves very differently from what is observed under ambient conditions. The significantly lowered viscosity, for example, increases the solubility as well as the diffusion rate of the solid reagents, therefore enhancing the crystal growth. The technique has been commonly employed in the synthesis of numerous solid-state inorganic materials. Comparably, it is relatively unexplored in the area of coordination compounds.² Recently, we have initiated a program focusing on single-crystal growth of coordination polymers of one-, two- and three-dimensional networks using the hydrothermal approach.^{3–7} Although simple transition-metal dihalide $4,4'$ -bipyridine ($4,4'$ -bpy) adduct complexes were first

investigated nearly 30 years ago,^{8,9} most of them were obtained as polycrystalline samples and were insoluble in common organic solvents. This had made the structure analysis very difficult. The structures of these compounds were thus proposed mainly on the basis of the IR data or for few by powder X-ray diffraction at a later time.¹⁰ While several other techniques failed to produce suitably sized crystals, we have explored the possibility of growing single crystals of metal dichloride $4,4'$ -bpy adducts by hydrothermal reactions. We have focused on the systems containing magnetically active metal centers, since strong magnetic exchange interactions are expected in these systems through relatively closely placed metal species ($\sim 3.6 \text{ \AA}$). Studies on magnetic properties have been reported on a number of compounds that are structurally related to metal dichloride $4,4'$ -bpy adducts, including $\text{MCl}_2 \cdot 2\text{H}_2\text{O}$ ($\text{M} = \text{Fe}$ and

* Corresponding author. Fax: 856-225-6506. E-mail: jingli@crab.rutgers.edu.

- (1) Ludise, R. A. In *Progress in Inorganic Chemistry*; Interscience Publishers: New York, 1962; Vol. III. Rabenau, A. *Angew. Chem., Int. Ed. Engl.* **1985**, 24, 1026. Laudise, R. A., *Chem. Eng. News* **1987**, September 28, 30.
- (2) See for example, Gutschke, S. O. H.; Slawin, A. M. Z.; Wood, P. T. *J. Chem. Soc., Chem. Commun.* **1995**, 2197. Yaghi, O. M.; Li, H. *J. Am. Chem. Soc.* **1996**, 117, 10401. Gutschke, S. O. H.; Molinier, M.; Powell, A. K.; Winpenny, E. P.; Wood, P. T. *Chem. Commun.* **1996**, 823. Yaghi, O. M.; Li, H. *J. Am. Chem. Soc.* **1996**, 118, 295.
- (3) Lu, J. Y.; Cabrera, B. R.; Wang, R.-J.; Li, J. *Inorg. Chem.* **1998**, 37, 4480.

- (4) Cabrera, B. R.; R.-J. Wang; Li, J.; Yuen, T. In *Solid State Chemistry of Inorganic Materials II*; ISBN 1-55899-453-X, 1999; Vol. 547, pp 493–498.
- (5) Lu, J. Y.; Cabrera, B. R.; Li, J. *Inorg. Chem.* **1999**, 38, 2695.
- (6) Lu, J. Y.; Cabrera, B. R.; R.-J. Wang; Li, J. *Inorg. Chem.* In press.
- (7) Pan, L.; Huang, X.-Y.; Li, J.; Wu, Y.-G.; Zheng, N.-W. *Angew. Chem., Int. Ed. Engl.* Submitted. Pan, L.; Huang, X.-Y.; Li, J. *Chem. Commun.* submitted.
- (8) Musgrave, T. R.; Mattson, C. E. *Inorg. Chem.* **1968**, 7, 1433.
- (9) Ferraro, J. R.; Davis, K. C. *Inorg. Chim. Acta* **1969**, 3, 685.
- (10) Masciocchi, N.; Cairati, P.; Carlucci, L.; Mezza, G.; Ciani, G.; Sironi, A. *J. Chem. Soc., Dalton Trans.* **1996**, 2739.

Co),^{11–14} M(pyridine)₂Cl₂ (M = Fe, Co, and Ni),^{15–17} and [(CH₃)₃NH]CoCl₃·2H₂O,¹⁸ all containing polymeric chains of (–MCl₂–) units. Investigation of the title compounds may reveal some interesting features regarding the magnetic ordering temperature and the type of the ground state ordering for single and mixed metal systems, thus providing further test of the theoretical models used in earlier studies of the MCl₂ chain compounds. Herein we report the details of the synthesis, crystal structure analysis by both single crystal and powder X-ray diffraction techniques, and the magnetic properties of ²[MCl₂(bpy)], M = Fe, Co, Ni, Co/Ni, a two-dimensional coordination polymer containing magnetic metal centers. The thermal stability of these compounds is assessed by thermogravimetric analysis.

Experimental Section

Chemicals and Reagents. All chemicals used are as purchased without purification: FeCl₂ (99.5%, Alfa Aesar), FeCl₂·4H₂O (99+%, ACROS), FeCl₃ (98%, Strem), CoCl₂ (99.7%, Alfa Aesar), CoCl₂·6H₂O (98%, ACROS), NiCl₂ (99%, Alfa Aesar), NiCl₂·6H₂O (97%, ACROS), oxalic acid (H₂C₂O₄·2H₂O, 97%, Alfa Aesar), 4,4'-bipyridine (98%, Alfa Aesar). Water is used as a solvent in all reactions.

Synthesis of ²[FeCl₂(bpy)] (I). Brownish crystals of **I** were obtained from reactions of FeCl₃ (0.1622 g), H₂C₂O₄·2H₂O (0.1261 g), bpy (0.1562 g), and H₂O (5 mL) in the mole ratio of 1:1:1:278. The reactions were carried out in a 23 mL acid digestion bomb at 170 °C for 7 days. The product was washed with water and acetone and dried in air. Columnlike crystals of **I** were collected (76% yield). Subsequent reactions in attempts to obtain single-phased samples were carried out using both FeCl₂ and FeCl₃. Powder XRD analysis indicated formation of Fe₂O₃ in the case of stoichiometric mixing of FeCl₂·4H₂O (0.1988 g) and bpy (0.1562 g). Single-phased **I** was obtained only when FeCl₃ was used as reagent in the presence of oxalic acid.

Synthesis of ²[CoCl₂(bpy)] (II). Crystals of **II** were grown from reactions of CoCl₂·6H₂O (0.1189 g), H₂C₂O₄·2H₂O (0.063 g), bpy (0.0781 g), and H₂O (8 mL) in the mole ratio of 1:1:1:889. The reactions were heated in 23 mL acid digestion bombs at 170 °C for 7 days. The product was washed with water and acetone and dried in air. Pale pink-purple crystals of **II** were isolated along with crystals of ²[Co(oxa)(bpy)].⁵ Subsequent reactions using a stoichiometric mixture of CoCl₂ (0.1298 g) and bpy (0.1562 g) in water (H₂O, 8 mL) at 170 °C for 3 days produced a single-phased pale pink-purplish polycrystalline sample of **II** (70% yield).

Synthesis of ²[NiCl₂(bpy)] (III). Similar reactions using NiCl₂ (0.1296 g), bpy (0.1562 g), and H₂O (4 mL) in the mole ratio of 1:1:444 in a 23 mL acid digestion bomb at 170 °C for 3 days resulted in single-phased pale green-yellowish polycrystalline samples of **III** (72% yield).

Synthesis of ²[(Co/Ni)Cl₂(bpy)] (IV). Single-phased, polycrystalline pale grayish samples of **IV** (70% yield) were obtained from hydrothermal reactions containing 0.1190 g of CoCl₂·6H₂O, 0.1198 g of NiCl₂·6H₂O, 0.1562 g of bpy, and 8 mL of H₂O (mole ratio of 1:1:1:444). The same product was obtained with anhydrous metal chlorides as reagents. The same reaction conditions were applied as described for the synthesis of **I–III**.

Table 1. Crystallographic Data for **I** and **II**

	I	II
empirical formula	C ₁₀ H ₈ Cl ₂ FeN ₂	C ₁₀ H ₈ Cl ₂ CoN ₂
fw	282.93	286.01
a, Å	11.929(2)	11.993(2)
b, Å	11.447(2)	11.374(2)
c, Å	3.638(1)	3.611(1)
V, Å ³	496.77(18)	492.57(18)
Z	2	2
space group	Cmmm (No. 65)	Cmmm (No. 65)
T, K	293(2)	293(2)
λ, Å	0.71073	0.71073
ρ _{calc} , g cm ^{−3}	1.891	1.928
μ, mm ^{−1}	2.015	2.243
R1 ^a (I > 2σ(I))	0.0522	0.0667
wR2 ^b	0.1136	0.1062

^a R1 = $\sum ||F_o| - |F_c|| / \sum |F_o|$. ^b wR2 = $[\sum (F_o^2 - F_c^2)^2 / \sum wF_o^4]^{1/2}$. Weighting: **I**, $w = 1/[\sigma^2(F_o^2) + 6.0P]$, where $P = (F_o^2 + 2F_c^2)/3$; **II**, $w = 1/[\sigma^2(F_o^2)]$.

Table 2. Atomic Coordinates and Equivalent Isotropic Temperature Factors (Å²) for **I** and **II**

atoms	x	y	z	U(eq) ^a
I				
Fe	0	0	0	0.016(1)
Cl	0.1443(2)	0	0.5000	0.019(1)
N	0	0.1908(8)	0	0.020(2)
C(1)	0.0916(7)	0.2529(8)	0	0.063(4)
C(2)	0.0854(7)	0.3728(8)	0	0.069(5)
C(3)	0	0.4355	0	0.020(2)
H(1)	0.1576	0.2156	0	0.076
H(2)	0.1665	0.4121	0	0.082
II				
Co	0	0	0	0.036(1)
Cl	0.1426(2)	0	0.5000	0.033(1)
N	0	0.1892(8)	0	0.041(3)
C(1)	0.0921(7)	0.2517(8)	0	0.101(6)
C(2)	0.0967(9)	0.3699(7)	0	0.085(5)
C(3)	0	0.4354(10)	0	0.034(2)
H(1)	0.1581	0.2144	0	0.121
H(2)	0.1679	0.4092	0	0.102

^a U(eq) is defined as one-third of the trace of the orthogonalized U_{ij} tensor.

Crystallographic Studies. A brownish blocklike crystal of **I** (0.06 × 0.08 × 0.13 mm) and a pale pink-purplish columnlike crystal of **II** (0.04 × 0.06 × 0.20 mm) were selected for structure analysis. Each crystal was mounted on a glass fiber in air on an Enraf-Nonius CAD4 automated diffractometer. The unit cell parameters for data collection were measured from least-squares analysis of the setting angles of 25 well-centered reflections in each case. All data were collected using graphite-monochromated Mo Kα radiation at 293(2) K with ω-scan method within the limits 5° ≤ 2θ ≤ 52° (**I**) and 7° ≤ 2θ ≤ 50° (**II**). Raw data were corrected for Lorentz and polarization effects, and an empirical absorption correction¹⁹ was applied in each case. The structure was solved using the SHELX-97 program.²⁰ Analytic expressions of atomic scattering factors were employed, and anomalous dispersion corrections were incorporated.²¹ The non-hydrogen atoms were located by direct phase determination and subjected to anisotropic refinement. The hydrogen atoms were generated theoretically. The full-matrix least-squares calculations on F^2 were applied on the final refinements. The unit cell parameters, along with data collection and refinement details for both **I** and **II**, are given in Table 1. The final positional and isotropic thermal parameters of atoms are listed in Table 2, and selected bond lengths and angles are reported in Table 3. The structural factors and

- (11) Narath, A. *Phys. Rev. Sect. A* **1965**, *139*, 1221.
- (12) Cox, D. E.; Shirane, G.; Frazer, B. C.; Narath, A. *J. Appl. Phys.* **1966**, *37*, 1126.
- (13) Weitzel, H.; Schneider, W. *Solid State Commun.* **1974**, *14*, 1025.
- (14) Kandel, L.; Weber, M. A.; Frankel, R. B.; Abeledo, C. R. *Phys. Lett.* **1974**, *A 46*, 369.
- (15) Takeda, K.; Matsukawa, S.; Haseda, T. *J. Phys. Soc. Jpn.* **1971**, *30*, 1330.
- (16) Foner, S.; Frankel, R. B.; Reiff, W. M.; Little, B. F.; Long, G. J. *Solid State Commun.* **1975**, *16*, 159.
- (17) Foner, S.; Frankel, R. B.; Reiff, W. M.; Wong, H.; Long, G. J. *J. Chem. Phys.* **1978**, *68*, 4781.
- (18) Losee, D. B.; McElearney, J. N.; Shankle, G. E.; Carlin, R. L.; Cresswell, P. J.; Robinson, W. T. *Phys. Rev. B* **1973**, *8*, 2185.

- (19) Kopfmann, G.; Hubber, R. *Acta Crystallogr.* **1968**, *A24*, 348–351.
- (20) Sheldrick, G. M. SHELX-97: program for structure refinement: University of Goettingen: Germany, 1997.
- (21) *International Tables for X-ray Crystallography*; Kluwer Academic Publishers: Dordrecht, 1989; Vol. C, Tables 4.2.6.8 and 6.1.1.4.

Table 3. Selected Bond Lengths (Å) and Bond Angles (deg)

I		II	
Fe–N	2.184(9) 2×	Co(1)–N(1)	2.152(9) 2×
Fe–Cl	2.5042(17) 4×	Co(1)–Cl(1)	2.4869(19) 4×
N–C(1)	1.304(10) 2×	N(1)–C(1)	1.314(10) 2×
N–Fe–N	180.0	N–Co–N	180.0
N–Fe–Cl	90.0	N–Co–Cl	90.0
Cl–Fe–Cl	180.0, 93.17(8), 86.83(8)	Cl–Co–Cl	180.0, 93.10(9), 86.90(9)
Fe–Cl–Fe	93.17(8)	Co–Cl–Co	93.10(9)
C(1)–N–Fe	123.0(5)	C(1)–N(1)–Co(1)	122.7(5)

Table 4. Unit Cell Refinement Results (Å) for I–IV

cell	I	II	III	IV
<i>a</i>	11.945(4)	11.954(3)	11.972(2)	11.928(2)
<i>b</i>	11.455(5)	11.411(1)	11.332(2)	11.352(2)
<i>c</i>	3.651(1)	3.618(1)	3.583(1)	3.582(1)
ESD (%)	3.7	1.6	1.1	2.5

anisotropic displacement parameters are deposited as Supporting Information. Crystal drawings were generated by SCHAKAL 92.²²

Attempts to grow single crystals of **III** and **IV** suitable for structure analysis by single-crystal X-ray diffraction were not successful. The unit cells of these compounds were refined using the powder XRD data of single-phased samples. The refinement was also performed on **I** and **II** as a comparison. The powder diffraction analyses were performed on a Rigaku D/M-2200T automated diffraction system (Ultima⁺). All measurements were made in a 2θ range of 5° – 80° at the operating power of 40 kV/40 mA. The data were collected at room temperature with a step size of 0.005 – 0.01° and a scan speed of 0.6 – $0.8^\circ/\text{min}$. The refinement was performed using JADE (Windows) software package.²³ The refinement results, including those of **I** and **II**, are listed in Table 4.

Magnetic Measurements. Magnetic measurements on single-phased polycrystalline samples of **I**–**IV** were performed using a Quantum Design SQUID magnetometer. These measurements include the field dependent magnetization, $M(H)$, and magnetic susceptibility, $\chi(T)$, defined as $M(T)/H$. The temperature was varied in the $\chi(T)$ measurements from 2 to 350 K. For each compound, we performed both the zero-field-cooled (ZFC) and field-cooled (FC) measurements of $\chi(T)$ under several magnetic fields. $M(H)$ was measured at 2 K for all samples. The applied magnetic field was increased from 0 to 5.4 T and then decreased back to 0 T.

Thermal Analysis. Thermogravimetric (TGA) analyses were performed on a computer-controlled TA Instrument 2050TGA analyzer. Powder samples of **I** (23.424 mg), **II** (20.832 mg), **III** (13.369 mg), and **IV** (19.686 mg) were loaded into alumina pans and heated from room temperature to 800°C (ramp rate of $10^\circ\text{C}/\text{min}$).

Results and Discussion

Structures. Compounds **I**–**IV** are isostructural and belong to the orthorhombic crystal system, space group $Cmmm$ (No. 65). As shown in Figure 1 (top), the crystal structure of **I**–**IV** consists of two-dimensional $[\text{MCl}_2(\text{bpy})]$, ($\text{M} = \text{Fe}, \text{Co}, \text{Ni}, \text{Co/Ni}$) networks built upon $\text{MCl}_4(\text{bpy})_2$ building blocks. The divalent metal centers have a distorted octahedral coordination with four $\mu_2\text{-Cl}$ and by two bridging 4,4'-bpy at trans positions (trans- D_{4h}). The 2D layers are formed in the ac plane by connecting metal centers via bridging chlorine and 4,4'-bpy ligands. These layers stack on top of each other along the b -axis at a distance of $1/2b$ to complete the three-dimensional structure (Figure 1, bottom).

The single Fe–Cl and Co–Cl distances, 2.504(2) and 2.487(2) Å, respectively, are comparable with those found in

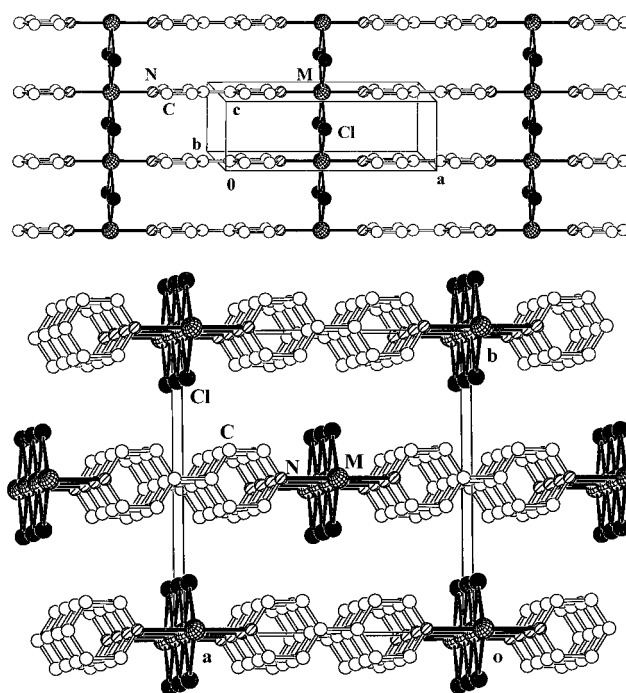


Figure 1. Two-dimensional network of $[\text{MCl}_2(\text{bpy})]^{2-}$. Top: view along the b -axis showing a single layer. Bottom: view along the c -axis showing stacks of layers. The cross-shaded circles are M ($\text{M} = \text{Fe}, \text{Co}, \text{Ni}, \text{Co/Ni}$), open circles are C, solid circle are O, and shaded circles are N.

molecular $\text{Fe}_4\text{Cl}_8(\text{C}_4\text{H}_8\text{O})_6$ (av Fe–($\mu_2\text{-Cl}$) = 2.451 Å),²⁴ $\text{Co}_4\text{-Cl}_8(\text{C}_4\text{H}_8\text{O})_6$ (av Co–($\mu_2\text{-Cl}$) = 2.400 Å),²⁵ $\text{Fe}_2\text{Cl}_3(\text{C}_4\text{H}_8\text{O})_6$ (av Fe–($\mu_2\text{-Cl}$) = 2.488 Å),²⁶ and $\text{Co}_3\text{Cl}_8(\text{C}_4\text{H}_8\text{O})_2$ (av Co–($\mu_2\text{-Cl}$) = 2.403 Å),²⁷ and polymeric $[\text{FeCl}_2(\text{H}_2\text{O})_2][(\text{HN}(\text{CH}_3)_3\text{Cl})]$ (av Fe–($\mu_2\text{-Cl}$) = 2.514 Å),²⁸ $[\text{CoCl}_2(\text{H}_2\text{O})_2][(\text{HN}(\text{CH}_3)_3\text{Cl})]$ (av Co–($\mu_2\text{-Cl}$) = 2.480 Å),²⁹ and $[\text{Fe}_2\text{Cl}_4(\text{OP}(\text{CH}_3)_3)_2]$ (av Fe–($\mu_2\text{-Cl}$) = 2.451 Å).³⁰ All N–M–Cl and N–M–N angles are precisely 90° and 180° , respectively. The M–M distances within the 2D net are the same as c (3.58–3.62 Å) and a (11.33–11.41 Å), respectively. While the distances along the a direction are too long for any significant magnetic interactions, relatively strong magnetic exchange interactions along the c direction may be anticipated for all compounds. Such interactions will be discussed in the following section.

- (22) Keller, E. SCHAKAL 92: a computer program for the graphical representation of crystallographic models: University of Freiburg: Germany, 1992.
 (23) JADE for Windows: XRD Pattern Processing for the PC, 1991–1995 Materials Data, Inc.

- (24) Cotton, F. A.; Luck, R. L.; Son, K.-A. *Inorg. Chim. Acta* **1991**, 179, 11.
 (25) Sobota, P.; Olejnik, Z.; Utako, J.; Lis, T. *Polyhedron* **1993**, 12, 613.
 (26) Janas, Z.; Sobota, P.; Lis, T. *J. Chem. Soc., Dalton Trans.* **1991**, 2429.
 (27) von Hahnisch, C.; Fenske, D.; Weigend, F.; Ahlrichs, R. *Chem.* **1997**, 3, 1494.
 (28) Greeney, R. E.; Landee, C. P.; Zhang, J. H.; Reiff, W. M. *Phys. Rev. B* **1989**, 39, 12200.
 (29) Losee, D. B.; McElearney, J. N.; Shankle, G. E.; Carlin, R. L. *Phys. Rev. B* **1973**, 8, 2185.
 (30) Cotton, F. A.; Luck, R. L.; Son, K.-A. *Inorg. Chim. Acta* **1991**, 184, 177.

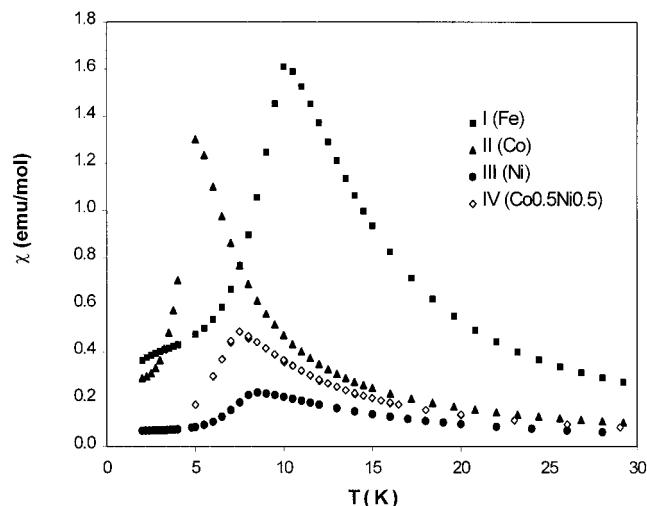


Figure 2. Magnetic susceptibility $\chi(T)$ measured in an applied field of 1 kG on polycrystalline samples of **I–IV**, for the low-temperature range.

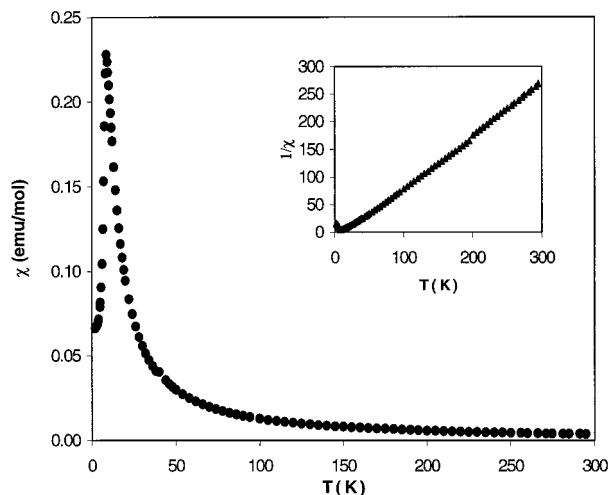


Figure 3. Magnetic susceptibility $\chi(T)$ measured in an applied field of 1 kG on a polycrystalline sample of **III**. Inserted is a plot of $1/\chi(T)$ vs T data.

Magnetic Properties. Our data for the low-field ($H < 0.2$ T) magnetic susceptibility of all four compounds revealed spontaneous magnetic orderings at low temperatures. The $\chi(T)$ data for **I–IV** in the low-temperature region are plotted in Figure 2. The transition temperatures for **I–IV** are 10, 5, 8.5, and 7.5 K, respectively. Figure 3 shows the susceptibility curve of $\chi(T)$ for **III** in the full temperature range, with $1/\chi(T)$ plot as an inset. Above the transition temperatures, the $\chi(T)$ data were fit to a modified Curie–Weiss law, $\chi(T) = \chi_0 + C/(T + \theta)$. By fitting the data we obtained the effective magnetic moment values, defined as $\mu_{\text{eff}} = 2.83 (C)^{1/2} \mu_B$, to be 5.7, 4.5, 3.0, and 3.8 μ_B , for **I**, **II**, **III**, and **IV**, respectively. These μ_{eff} values indicate a high spin state for each M(II) ion. The cusplike low temperature $\chi(T)$ data of all the samples suggest antiferromagnetic orderings. However, the fitted θ values for all compounds are positive, thus indicating more complicated magnetic interactions among the M ions in these compounds.

The field dependent magnetization, $M(H)$, measured at 2 K for **I–IV** are shown in Figure 4. Hysteresis was found in $M(H)$ measurements of all samples, with that of the compound **III** being the most significant. In the low-field region, the $M(H)$ curves are linear, consistent with the antiferromagnetic behavior of $\chi(T)$ shown in Figures 2 and 3. But as the field increases,

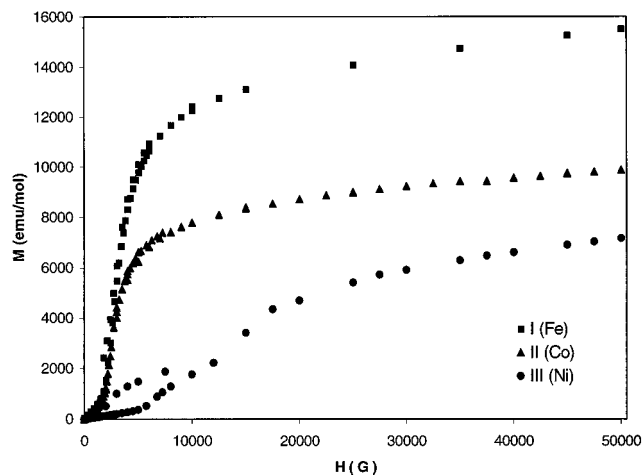


Figure 4. Magnetization measured at 2 K for samples of **I–III**.

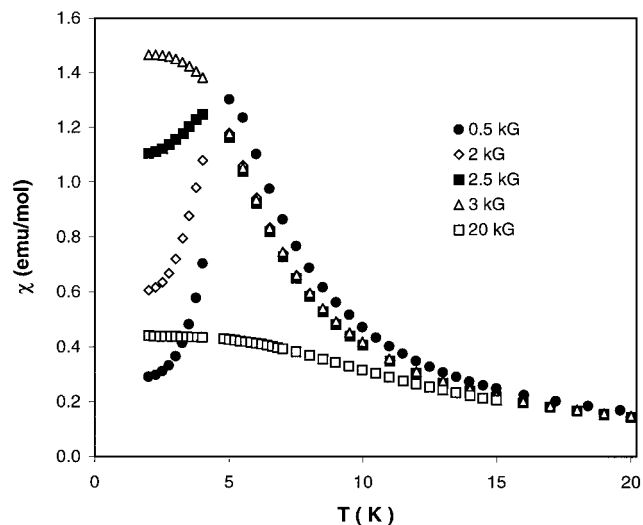


Figure 5. Magnetic susceptibility $\chi(T)$ measured under different fields on **II**.

the $M(H)$ curves start to increase their slopes above a critical field, H_C , and then become somehow saturated at the high-field region. At 50 kG, moments of $2.76 \mu_B$ for **I** and $1.79 \mu_B$ for **II** were obtained. The $M(H)$ curves for **III** and **IV** are less saturated and moments of $1.28 \mu_B$ for **III** and $1.56 \mu_B$ for **IV** were measured at 50 kG. Figure 5 shows the $\chi(T)$ data for **II**, measured under several fields. The transition temperature, T_N (determined as the temperature at which $\chi(T)$ reaches peak value), is suppressed by the field from 5 K for 500 G data, to 4 K for 2.5 kG data, and under $H > 3$ kG, the $\chi(T)$ shows no clear transitions. The studies of $\chi(T)$ under different fields for other three compounds also showed similar effects.

The $\chi(T)$ and $M(H)$ data of the $\text{MCl}_2(4,4'\text{-bpy})$ system exhibited a typical metamagnetic behavior in that the ground-state magnetic structure changes upon the change in the applied field. Below a critical field, H_C , the ground-state magnetic structure is antiferromagnetic. When the applied field is stronger than H_C , the ground state is ferromagnetic-like or paramagnetic-like. The critical field, determined as the field under which the cusp in $\chi(T)$ measurement disappears, for **I**, **II**, **III**, and **IV** are 3.5, 2.5, 12, and 7 kG, respectively. The metamagnetic transitions observed in the $\text{MCl}_2(4,4'\text{-bpy})$ series resemble that found in the similar chain systems $\text{MCl}_2 \cdot 2\text{H}_2\text{O}$ ($\text{M} = \text{Fe}$ and Co),^{11–14} and $\text{M}(\text{pyridine})_2\text{Cl}_2$ ($\text{M} = \text{Fe}$, Co , and Ni).^{15–17} However, the critical fields for the title compounds are much lower than that

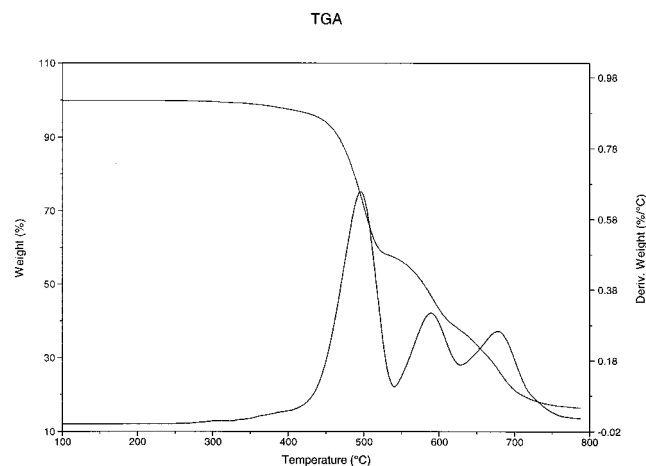


Figure 6. Thermogravimetric analysis (TGA) data showing weight loss of **I** as a function of temperature between 100 and 800 °C. The negative of the first derivative (%/°C) is also plotted as a function of temperature.

in the $\text{MCl}_2 \cdot 2\text{H}_2\text{O}$ and close to that found in the $\text{M}(\text{pyridine})_2\text{Cl}_2$ systems.

As discussed in the above section, the magnetic divalent metal centers in $\text{MCl}_2(4,4'\text{-bpy})$ compounds sit in a distorted octahedral environment with four Cl and two 4,4'-bpy. The Cl–M–Cl angles are close to, but deviated from, 90°. The M–Cl bonds are about 2.5 Å. The one-dimensional magnetic interaction is achieved through the M–Cl₂–M exchange pathway. Because Anderson's superexchange theory³¹ predicts a favored ferromagnetic exchange for a 90° interaction pathway, it is anticipated that the M–M intrachain exchange interaction through the Cl₂ bridges in our $\text{MCl}_2(4,4'\text{-bpy})$ system is ferromagnetic, and the antiferromagnetic coupling is originated from the M–M interchain interaction. Such a proposed model for the magnetic structures of $\text{MCl}_2(4,4'\text{-bpy})$ system is consistent with our experimental data. Other complementary and further magnetic measurements on single crystals are being conducted to confirm the proposed model.

Thermal Stability. Depicted in Figures 6 and 7 are results from thermogravimetric analyses performed on **I** and **II**. Compounds **III** and **IV** show similar behavior as **II** upon heating. The weight losses observed for **I** and **II**, along with the negative values of the first derivatives (%/°C) are plotted as functions of temperature between 100 and 800 °C (**I**) and between 50 and 750 °C (**II**). All four compounds are thermally stable up to 400 °C. Compound **I** underwent a three-step decomposition process, while **II–IV** showed a two-step weight-loss mechanism, as seen clearly from the first-derivative plots. In all cases, the loss of 4,4'-bpy and chlorine was completed before the temperature reached 800 °C. Subsequent powder XRD analysis identified elemental metals (Fe, Co, Ni) as the only residues. The demonstrated thermal stability of the title

(31) Anderson, P. W. In *Magnetism*; Rado, G. T., Suhl, H., Eds.; Academic: New York, 1963; Vol. 1, Chapter 2.

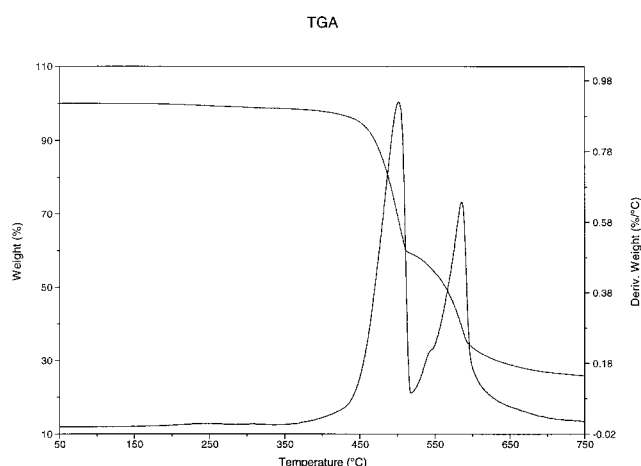


Figure 7. Thermogravimetric analysis (TGA) data showing weight loss of **II** as a function of temperature between 50 and 750 °C. The negative of the first derivative (%/°C) is also plotted as a function of temperature.

compounds may be attributed to the π – π interactions between the adjacent parallel bpy rings stacking along the *c*-axis. The similar π – π interactions have also been observed in a number of coordination compounds containing aromatic rings.^{5,32}

Conclusions

A family of metal chloride 4,4'-bpy adduct complexes $[\text{MCl}_2(\text{bpy})]_2$, M = Fe, Co, Ni, Co/Ni, have been synthesized via hydrothermal routes with relatively high yields. The crystal structures of these compounds have been analyzed by both single crystal and powder X-ray diffraction methods. These compounds possess a two-dimensional crystal structure and exhibit spontaneous magnetic ordering and metamagnetic transition. All four compounds are stable up to >400 °C, due likely to the π – π interaction between the adjacent (parallel) bipyridine rings. The magnetic property studies suggest that the metal–metal intrachain exchange interaction is ferromagnetic, while the metal–metal interchain coupling is antiferromagnetic.

Acknowledgment. Financial support from the National Science Foundation (DMR-9553066) is greatly appreciated. The TGA/DSC analyzer was purchased through a NSF ARI grant (CHE 9601710-ARI).

Supporting Information Available: Tables of atomic coordinates of all atoms, isotropic and anisotropic thermal parameters, bond distances and angles, crystallographic data and ORTEP drawings for compounds **I** and **II** (11 pages). This material is available free of charge via the Internet at <http://pubs.acs.org>.

IC990286C

(32) Yaghi, O. M.; Li, G.-M.; Li, H.-L. *Nature* **1995**, 378, 703. Hartshorn, C. M.; Steel, P. J. *Inorg. Chem.* **1996**, 35, 6902. Coates, G. W.; Dunn, A. R.; Henling, L. M.; Dougherty, D. A.; Grubb, R. H. *Angew. Chem., Int. Ed. Engl.* **1997**, 36, 248; Dai, J.; Yamamoto, M.; Kuroda-Sowa, T.; Kaekawa, M.; Suenaga, Y.; Munakata, M. *Inorg. Chem.* **1997**, 36, 2688.